Rheology of cellulose-[DBNH][CO 2 Et] solutions and shaping into aerogel beads

Lucile Druel, Philipp Niemeyer, Barbara Milow, Tatiana Budtova

Green Chem., 20, 3993 – 4002 (2018) DOI: 10.1039/c8gc01189c

Rheology of cellulose-[DBNH][CO_2Et] solutions and shaping into aerogel beads

Lucile Druel[1], Philipp Niemeyer[2], Barbara Milow[2], Tatiana Budtova[1]*

[1] *MINES ParisTech, PSL Research University, Centre for Material Forming (CEMEF), UMR CNRS 7635, CS 10207, 06904 Sophia Antipolis, France*

[2] *Deutsches Zentrum für Luft- und Raumfahrt Institut für Werkstoff-Forschung, Abteilung Aerogele, Linder Höhe, 51147 Köln, Germany*

Corresponding author:

Tatiana Budtova, Tatiana.Budtova@mines-paristech.fr

Tel +33 4 93 95 74 70

Abstract

Cellulose aerogel beads were made with JetCutting technology and dried by supercritical CO_2 extraction. Ionic liquid, 1,5-diazabicyclo[4.3.0]non-5-enium propionate ([DBNH][CO_2Et]), was shown to be a suitable solvent due to its rheological and thermodynamic properties. The flow and viscoelastic properties of cellulose-[DBNH][CO_2Et] solutions were studied in detail as a function of polymer concentration and solution temperature and compared to those of cellulose-1-ethyl-3-methylimidazolium acetate ([Emim][OAc]). [DBNH][CO_2Et] is thermodynamically better solvent as cellulose intrinsic viscosity is more than two times higher than that in [Emim][OAc]. This allows simultaneously fitting i) the processing window of the JetCutter technology which requires rather low solution viscosity at high shear rates and ii) cellulose concentration being high enough above the overlap to make intact aerogel beads. The beads were prepared from 2 and 3 wt% cellulose-[DBNH][CO_2Et] solutions and coagulated in water, ethanol and isopropanol. Bead sizes were from 0.5 to 0.7 mm when made from 2% solutions and up to 1.7 mm when prepared from 3% solution. Cellulose aerogel beads prepared by JetCutting possessed main characteristics similar to those of monolithic cellulose aerogels obtained from cellulose dissolved in other solvents: the specific surface area was 240 – 340 $m^2.g^{-1}$ at densities of 0.04–0.07 $g.cm^{-3}$.

1. Introduction

Cellulose is an inexhaustible natural polymer; its use is reconsidered in our days due to the discoveries of non-toxic cellulose solvents and possibilities of making materials with various functionalities due to a large amount of reactive hydroxyl groups on anhydroglucose unit. Cellulose based aerogels are new and very promising materials offering a wide range of potential applications from bio-medical and cosmetics (delivery systems, scaffolds) to materials for adsorption and/or separation and electro-chemistry when pyrolysed.

Two main ways of making cellulose aerogels are known. The first is based on cellulose dissolution in a direct solvent resulting in cellulose II aerogels. Solvents used are 8% NaOH-water,[1,2] ionic liquids,[3–7] *N*-methyl-morpholine *N*-oxide (NMMO) monohydrate,[8,9] LiCl/dimethylacetamide[10], calcium thiocyanate tetrahydrate[11] and salt hydrate melts from zinc chloride.[12] To prevent pores' collapse during drying either lyophilisation[4,10,11] or drying with supercritical (sc) CO_2 [1–3,5,6,8,9,12] is used. The former usually leads to so-called cryogels with large pores due to ice crystals growth, resulting in very low densities, 0.05 – 0.1 $g.cm^{-3}$, but not very high specific surface area, 10-100 $m^2.g^{-1}$.[7,11] Supercritical drying with CO_2 much better preserves the structure of the network formed before drying (cellulose solvent is usually washed out by water or ethanol) leading to densities around 0.1 – 0.2 $g.cm^{-3}$ and specific surface areas ranging from 200 to 500 $m^2.g^{-1}$.[1,3,5,6,8,9] The reason is that in sc conditions capillary pressure, which develops during drying and is responsible for pores' collapse, is theoretically absent due to zero surface tension of the evaporating fluid. The overall characteristics of cellulose II aerogels are similar to those of other bio-aerogels from starch,[13] pectin,[14,15] alginate,[16,17] etc. It has to be noted that one of the advantages of cellulose, as compared to many other polysaccharides, is that it is temperature, pH and ion non-sensitive.

The second way of making cellulose aerogels is to use cellulose nanofibers, which can be either bacterial cellulose,[18] or micro- or nano-fibrillated cellulose, the latter prepared via mechanical disintegration of the native fibers,[19,20] often accompanied by the enzymatic and/or chemical treatment. In these cases the starting material is a continuous "non-woven" network of cellulose I nanofibers filled with water. Drying via lyophilisation results in cellulose I cryogels with density of 0.02 – 0.03 $g.cm^{-3}$ and specific surface area 50 – 100 $m^2.g^{-1}$.[19,21] When identical precursors are dried via sc route, the obtained cellulose I aerogels have density as low as 0.01 $g.cm^{-3}$ and surface area of 500-600 $m^2.g^{-1}$.[20] It should be noted that in addition to high porosity and high specific surface area, cellulose I and cellulose II aerogels offer numerous options of various functionalisations, making these materials versatile and targeted to different applications.

Until now, most of cellulose aerogels are produced in the form of monoliths which is simply due to easy preparation on laboratory scale. However, for many practical applications (food, cosmetics, medical, sorption and separation) the shape of beads with size varying from few microns to few millimeters, depending on the application, is preferable. Also, each processing step (solvent exchange, drying) is much faster with small beads as compared to monoliths which are usually of few cubic centimeters volume. Making cellulose beads is known since long time for immobilization, purification, separation and filtration purposes, however, in most of the cases they are used either in the "wet state" (never dried, usually in water) or, if dried, they are dried at ambient conditions which results in a non-porous material.

There are two general approaches for making cellulose II beads: i) dissolving a cellulose derivative (viscose, cellulose esters, or ethers), and then regenerating cellulose in a coagulation bath,[22–24] or ii) from cellulose solutions dissolved in direct solvents.[25–32] The techniques to make beads from cellulose solutions are either by using classical droplet-making machines like atomizers,[24,25] by dropping solution with a syringe,[2,26,27,30,32] by under-

water pelletisation,[31] or using emulsion method.[22,28,29] A recent review summarises various ways of production of cellulose beads.[33]

Very few is reported on the whole "chain" of making cellulose aerogel beads, from cellulose dissolution to bead shaping and to resulting aerogel properties. The majority of publications use simple "syringe-dropping" method to obtain beads. For example, using 7%NaOH-12%urea-water solvent, cellulose beads were made via dropping and their size, shape and surface area were modified by coagulation bath conditions.[27] Their volume in the wet state was 8 – 20 mm^3 and specific surface area after sc drying was 330 – 470 $m^2.g^{-1}$. The same solvent was used to make beads via emulsion method; in wet state their diameter varied from few microns to 1 mm and when freeze-dried, specific surface area was around 16 $m^2.g^{-1}$.[28] ZnO was added to this solvent, and aerogel beads were prepared using dropping technique; aerogel density varied from 0.08 to 0.25 $g.cm^{-3}$ and it was reported that specific surface area increased from 340 $m^2.g^{-1}$ without ZnO to 410 $m^2.g^{-1}$ with this additive.[30] Similar solvent, 8%NaOH-water, was also used to prepare cellulose aerogel beads via dropping method.[2] The shape varied from very flat plates to spheres; various inorganic powders were encapsulated into cellulose beads and organic-inorganic aerogel particles were prepared. Literature reports functionalised cellulose I porous cellulose beads, but the ways to prepare them are usually not detailed.

Even less is known on using ionic liquids for making cellulose aerogels in the form of beads. Ionic liquids are powerful cellulose solvents, with negligible vapour pressure, allowing cellulose derivatisation in homogeneous conditions[34] and spinning fibers from dissolved lignocellulose.[35] Ionic liquids have a strong advantage against NaOH-water based solvents: the latter do not allow the dissolution of high molecular weight cellulose and cellulose-NaOH-water solutions are irreversibly gelling with time and temperature increase.[36] Despite several advantages of ionic liquids as compared to other cellulose solvents, their recovery is not well

developed yet and is a recurrent topic in cellulose processing domain. Several methods were reported: from simple evaporation of cellulose non-solvent (water), to more complex solvent extraction[37] or phase separation.[38,39] Some ionic liquids were also proven to be distillable[40,41] and [DBNH][CO_2Et] is one of them. Its recyclability was demonstrated by Parviainen et al.[42] As far as cellulose aerogel beads are concerned, they were prepared by "syringe-dropping" of cellulose-1-allyl-3-methylimidozoiumchloride solution into water; particles of diameter from 0.4 to 2.2 mm were obtained and, surprisingly, specific surface area decreased from 500 to 100 m^2g^{-1}, respectively.[32]

The goal of this work is to demonstrate the feasibility of making cellulose II aerogel beads from cellulose-ionic liquid solutions, this being done using processing method which can be easily up-scaled. First, the rheological properties of cellulose-ionic liquid are investigated in details to validate the selection of ionic liquid and processing conditions. The ionic liquid selected is 1,5-Diazabicyclo[4.3.0]non-5-enium propionate ([DBNH][CO_2Et]) known to dissolve cellulose[42] and being liquid at room temperature. Classical polymer physics principles are used to interpret the results obtained. Cellulose aerogel beads were then prepared using the JetCutter technology and characterised by aerogel standards.

2. Materials and methods

2.1. Materials

Microcrystalline cellulose (MC) Avicel PH-101 with a degree of polymerisation (DP) of 265 (determined according to ISO 5351 and Marx-Figini (1978) constant via dissolution in cupriethylenediamine) was purchased from Sigma-Aldrich. 1,5-Diazabicyclo[4.3.0]non-5-ene (DBN) was purchased from Fluorochem. Propionic acid (EtCO_2H) (purity > 99%) was from Fisher Scientific. 1-ethyl-3-methylimidazolium acetate ([Emim][OAc]) was purchased from

BASF. Absolute ethanol (purity > 99%) and isopropanol (purity > 99.5%) were purchased from Fisher Chemicals. Water was distilled. All chemicals were used as received.

2.2. Methods

2.2.1. Ionic liquid and cellulose solutions preparation

The ionic liquid, 1,5-Diazabicyclo[4.3.0]non-5-enium propionate ([DBNH][CO_2Et]), was prepared before each experiment to prevent any influence of aging. EtCO_2H and DBN were mixed in a 1:1 molar ratio according to procedure described in ref. 42: EtCO_2H was slowly added to DBN under nitrogen atmosphere and 400 rpm magnetic stirring, in an ice bath, as far as the reaction is exothermal. Temperature was controlled throughout the reaction so that it did not exceed 30 °C. Stirring was maintained at least 30 min after all EtCO_2H was added to insure a complete reaction. The ionic liquid obtained was transparent and slightly yellowish. [DBNH][CO_2Et] was characterised with ^{1}H NMR in DMSO-d_6 using Varian 300 MHz Unity spectrometer (Department of Chemistry, University of Helsinki); full and expanded spectra are shown in Figure S1 of the Supporting Information together with assigned peaks. The ^{1}H NMR data are consistent with those reported previously by Parviainen et al.[42,43]

Prior to use, MC was dried overnight under vacuum at 50 °C. It was then dissolved at various concentrations in [DBNH][CO_2Et] at 40 °C and 400 rpm stirring with a Heidolph RZR 50 overhead mixer for 24 h. Dried MC was also dissolved in [Emim][OAc] at 75 °C and 400 rpm stirring for 24 h.

All solutions were kept at room temperature, under nitrogen atmosphere, to prevent moisture and oxygen uptake. In the following, the concentrations will be given in weight percent (%) unless otherwise mentioned.

2.2.2. Rheological measurements

All rheological measurements were performed within 3 days after solution preparation on a Bohlin Gemini rheometer equipped with cone-plate geometry (4 ° - 40 mm) and a Peltier temperature control system. For steady state, shear rate was varied from 0.01 s^{-1} to 300 s^{-1} and temperature from 10 °C to 60 °C. For dynamic mode, frequency sweeps were performed between 0.01 Hz and 10 Hz at 5 Pa which corresponds to the linear viscoelastic regime, with temperature also varying from 10 °C to 60 °C. To prevent moisture and oxygen uptake, a thin layer of low-viscosity silicon oil ($\eta_{20°C}$ = 9.5 mPa.s) was disposed on the edge of the measuring cell.

2.2.3. Cellulose aerogel beads

Cellulose aerogel beads were prepared via the dissolution-solvent exchange/coagulation-sc CO_2 drying route. Cellulose concentration in [DBNH][CO_2Et] was 2% and 3%. We used a JetCutter Type S from GeniaLab®, Germany, for the shaping. Pictures of the JetCutter and its tools are shown in Figure S2 of the Supporting Information. The principle of the JetCutter consists of cutting a jet of solution with high speed rotating wires. The jet cut into "cylinders" form spheres due to surface tension and are collected in a bath (here, three cellulose non-solvents were used: water, ethanol and isopropanol). Solvent in cellulose beads was washed out with non-solvent by several exchanges with the fresh one leading to non-solvent induced phase separation (or coagulation) of cellulose. The goal was to stabilise the shape of cellulose beads. If the non-solvent of the coagulation bath was not ethanol, it was then exchanged to ethanol and washed several times until the electrical conductivity of the ethanol bath was below 8.1 µS.cm^{-1}. Ethanol was selected because of its good miscibility with CO_2. Cellulose-ethanol beads were then dried in a custom made 12 L autoclave from Eurotechnika, Germany. Process conditions of the sc CO_2 were 115 bar and 60 °C. Dynamic washing with sc CO_2 was performed at flow rates around 15 kg/h for two hours before the extractor was depressurized at rates not lower than 1.5 bar/min and not higher than 3 bar/min.

2.2.4. Aerogels characterisation

The density ρ_{bulk} of aerogels was measured with a Micromeritics Geopyc 1360 powder densitometer, with DryFlo powder. The chamber was 19.1 mm diameter, and the force applied was 25 N. The error was less than 10%.

In order to build size distribution of cellulose aerogel beads, their images were taken with an Epson Perfection V550 Photo Color Scanner in transmission mode, in 8-bits greyscales with a 6400 dpi resolution (4 µm.pixel^{-1}). The images obtained were then analysed with the ImageJ software: the segmentation of the image was adjusted manually with a fixed grey level threshold to differentiate each bead from the background. Using "Analyse particles" tool of ImageJ, the beads were labelled, and their surface area measured. The beads were considered spherical in the first approximation and their diameter was calculated from the area. For each formulation at least 100 beads were analysed.

The morphology of aerogels was studied with a Supra40 Zeiss SEM FEG (Field Emission Gun). The observations were done with a diaphragm of 20 µm diameter and the acceleration voltage was set between 1 kV and 3 kV. Prior to the observations, a 7 nm layer of platinum was applied on the surface of the samples with a Q150T Quarum metallizer to prevent the accumulation of electrostatic charges.

The specific surface area (S_{BET}) was measured with an ASAP 2020 from Micromeritics using nitrogen adsorption and BET method. The samples were degassed under high vacuum at 70 °C for 10 h prior to measurements; the error was within ± 20 m^2/g.

3. Results and discussion

The first part of this section is devoted to the rheological study of cellulose-[DBNH][CO_2Et] solutions, and the second to the preparation of cellulose aerogel beads made with JetCutter technology and their characterisation.

The understanding of the viscoelastic properties of cellulose solutions is dictated, on one hand, by the use of JetCutter which has a certain processing window in terms of solution viscosity, and, on the other hand, by the need in using cellulose solutions of concentration which is at least 3 times higher than the overlap concentration, C*. The latter criterion is somehow evident as far as a self-standing cellulose network should be formed, and it was confirmed when making monolithic cellulose aerogels from cellulose-[Emim][OAc][6,7] and cellulose-8%NaOH-water solutions.[44]

Cellulose-[Emim][OAc] solutions of viscosities around and above 5-10 Pa.s turned out to be difficult to process with JetCutter. This was the case of 5% cellulose-[Emim][OAc] which is a typical low concentration for making aerogels when using microcrystalline cellulose.[7] There are several ways to overcome the problem of "too high" viscosity. One is simply to decrease cellulose concentration. However, when microcrystalline cellulose is dissolved in [Emim][OAc] at 2-3%, the network formed upon coagulation in non-solvent is very weak, and the beads are either not intact or highly deformed. The reason is that these concentrations are too close to cellulose C* which in [Emim][OAc] is around 1% at room temperature[45] (the same cellulose was used in the present work and in ref. 45). A compromise between not too high solution viscosity and not too low cellulose concentration (not too close to C*) is thus needed. To decrease the overlap concentration can be possible by using cellulose of higher molecular weight but viscosity increase will be more pronounced than the decrease in C*. The second way to decrease viscosity is to increase temperature but the JetCutter Type S is not adapted to this option. The third way is to use so-called co-solvents, for example, dimethylsulfoxide.[46,47] However, this approach has several drawbacks such as complications during solvent recovery and presence of undesirable traces. The "ideal" solvent should be with a) lower viscosity than [Emim][OAc] and, b) if possible, better thermodynamic quality as compared to [Emim][OAc]. The former would decrease solution viscosity, and the latter

would decrease C* allowing having stable cellulose network at lower polymer concentrations. Below we shall demonstrate that this is the case of [DBNH][CO_2Et]. Based on the results obtained with the rheological study, the preparation and properties of cellulose aerogel beads are then described.

3.1. Cellulose-[DBNH][CO_2Et] rheological properties

3.1.1. Solvent and solution aging

First of all, we examined the influence of temperature and time on solvent and solution viscosity as far as visual observations showed the darkening of solutions in time. Therefore, the evolution of viscosity of [DBNH][CO_2Et] at 20 °C was followed after shearing from 0.01 s^{-1} to 300 s^{-1} for 7 min at 40 °C and at 60 °C. The viscosity slightly increased but was within the 10% experimental errors. Yet, the influence of aging on cellulose-[DBNH][CO_2Et] solutions was considerable: the viscosity of a 5% solution at 20 °C was 27.7 Pa.s and it doubled to 53.2 Pa.s after 2 months of storing at ambient conditions. The aging of the pure ionic liquid was not so important but still noticeable: the viscosity increased from 0.146 Pa.s to 0.165 Pa.s after 1.5 months and to 0.210 Pa.s after 3 months of storage at room temperature. We suppose that the reason is hydrolysis of ionic liquid, as suggested in ref.43. As specified in the Materials and methods section, all rheological experiments and preparations of cellulose beads were thus performed on freshly made solutions.

3.1.2. Flow curves

The flow of [DBNH][CO_2Et] and cellulose-[DBNH][CO_2Et] solutions at different concentrations and temperatures was investigated in steady state and in dynamic mode. The examples of steady state viscosity η as a function of shear rate and of elastic (G') and viscous

(*G''*) moduli as well as complex viscosity (η^*) as a function of frequency are shown in Figure 1 and Figure 2, respectively.

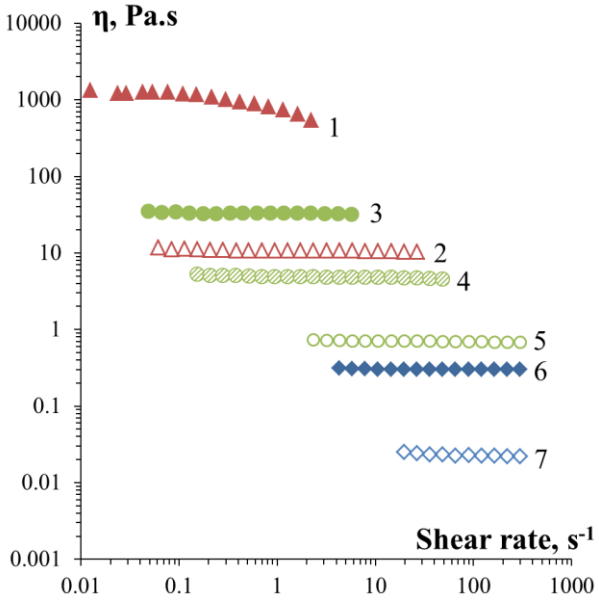

Figure 1.

Examples of flow curves for [DBNH][CO_2Et] and cellulose-[DBNH][CO_2Et] solutions at different concentrations and temperatures: 8% cellulose at 10 °C (1) and 60 °C (2), 4% cellulose at 10 °C (3), 30 °C (4) and 60 °C (5), neat [DBNH][CO_2Et] at 10 °C (6) and 60 °C (7).

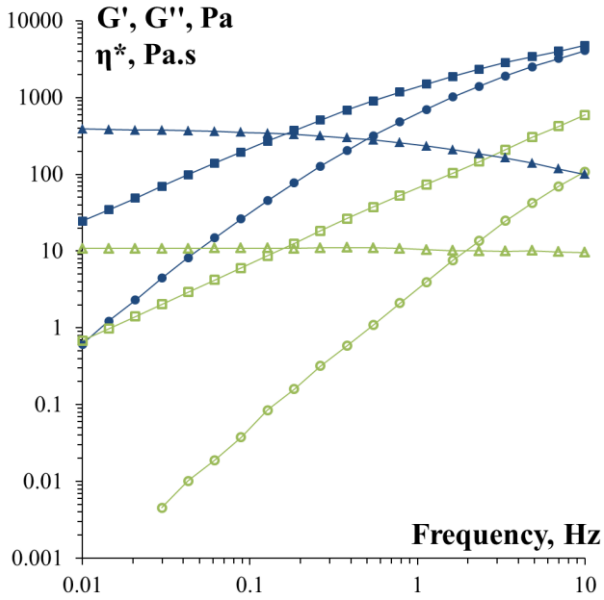

Figure 2.

Examples of *G'* (circles), *G"* (squares) and η^* (triangles) as a function of frequency. Filled points are measurements of 8% cellulose-[DBNH][CO_2Et] at 20 °C, open points are at 60 °C. Lines are given to guide the eye.

Figure 1 shows that the solvent and solutions have a Newtonian plateau for at least one or two decades of shear rates. Higher concentration and lower temperature lead to higher viscosity and a beginning of shear thinning. These results correlate with the behaviour of a classical polymer solution. The value of viscosity at the Newtonian plateau, the zero shear rate viscosity, will be used for the following analysis and referred as η_N. It should be noted that the viscosity of the neat solvent [DBNH][CO_2Et] at 20 °C is 0.145 Pa.s (not shown) and of [Emim][OAc] at the same temperature is 0.161 Pa.s.[45] Lower solvent viscosity is more favourable for processing with JetCutter. Figure 2 also shows typical behaviour of an un-entangled viscoelastic polymer solution, with $G" < G'$ over three decades of frequencies, from 0.01 to 10 Hz.

Because cellulose-[DBNH][CO_2Et] solutions show a classical polymer solution behaviour, we checked if Cox-Merz rule (which postulates the equality of steady state and dynamic

viscosities) is obeyed.[48] An example at 20 °C is presented in Figure 3 for three cellulose concentrations. It shows a very good match of η and η*; Cox-Merz rule can consequently be applied to cellulose-[DBNH][CO_2Et] solutions.

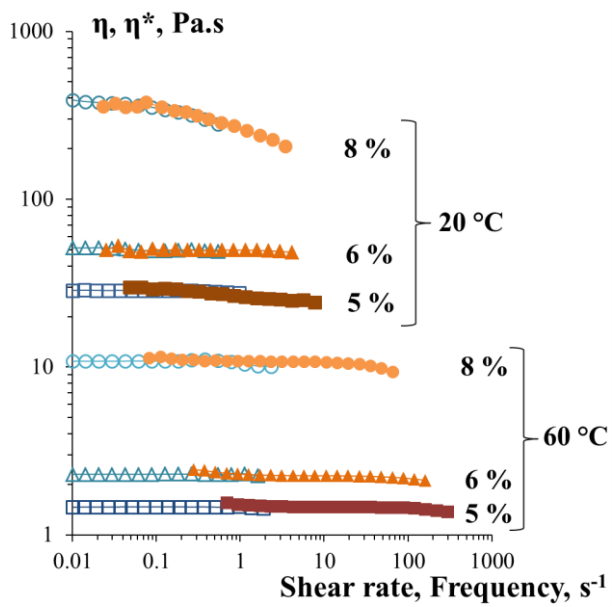

Figure 3.

Example of steady state viscosity (open points) and complex viscosity (filled points) curves of cellulose-[DBNH][CO_2Et] solutions at 20 and 60 °C and different concentrations, illustrating the Cox-Merz rule.

3.1.3. Activation energy and master curves

Arrhenius approach was used to correlate zero shear rate viscosity η_N and temperature T and calculate the activation energy E_a of viscous flow:

$$\eta_N \sim exp\left(\frac{E_a}{RT}\right) \quad (1)$$

where R is the ideal gas constant and temperature is expressed in K. The dependences of η_N of the solvent and cellulose solutions on inverse temperature are shown in Figure 4. They all show linear trends ($R^2 > 0.99$) allowing calculation of E_a at each cellulose concentration. It

was reported in previous works[345,49] that $ln(\eta_N)$ vs $1/T$ for [Emim][OAc] and cellulose-[Emim][OAc] solutions showed a concave shape, this being "dictated" by the ionic liquid. Even if a very weak trend can also be guessed for [DBNH][CO_2Et] and low concentrated cellulose-[DBNH][CO_2Et] solutions (Figure 4), the deviation from the linear dependence is within the experimental errors in the temperature interval studied.

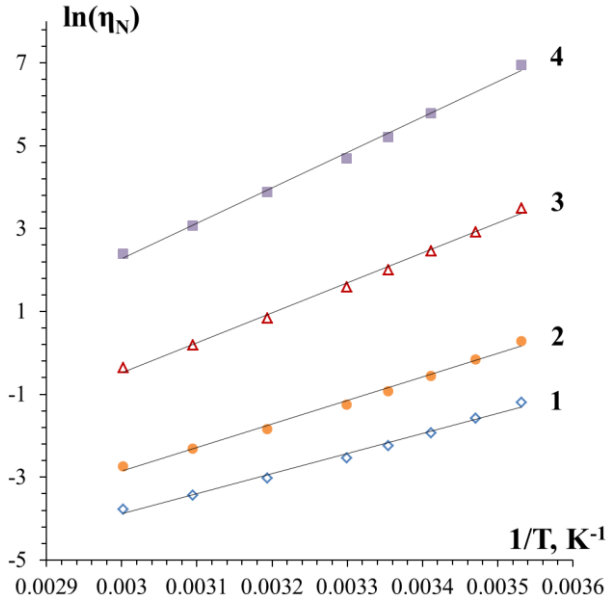

Figure 4.

Arrhenius plots of [DBNH][CO_2Et] (1) and cellulose-[DBNH][CO_2Et] solutions of 1% (2), 4% (3) and 8% (4). Lines are linear approximations.

The activation energies calculated using eq. 1 and data in Figure 4 are plotted as a function of cellulose concentration in Figure 5 and are shown together with the values for cellulose-[Emim][OAc] system taken from ref. 45. The power law approximations, given by eq. (2) which describes the activation energy as a function of polymer concentration, are also shown in Figure 5 with p = 8.22 and k = 0.60 for cellulose-[DBNH][CO_2Et] solutions and p = 3.21 and k = 0.83 for cellulose-[Emim][OAc] solutions.

$$E_a = E_a(0) + pC^k \quad (2)$$

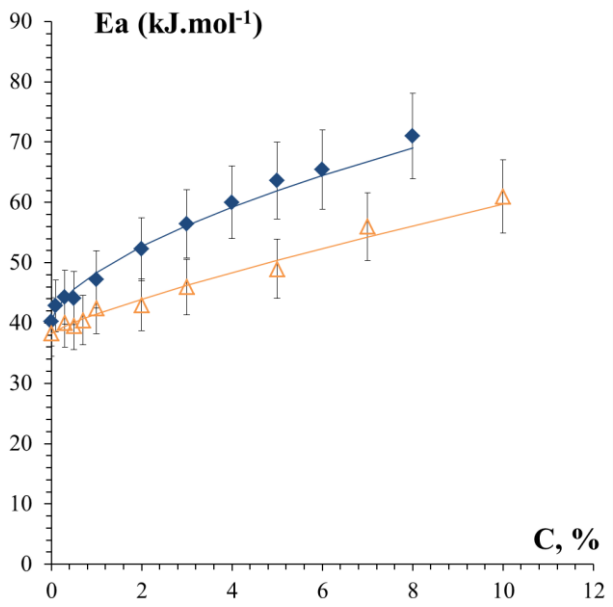

Figure 5.

Activation energy as a function of cellulose concentration for cellulose-[DBNH][CO_2Et] solutions (filled points) and cellulose-[Emim][OAc] solutions (open points). Solid lines correspond to approximations calculated with eq.(2).

While the activation energy of the neat solvents are almost the same, E_a of cellulose-[DBNH][CO_2Et] solutions is higher than that of cellulose-[Emim][OAc] solutions at all concentrations. This shows that the viscosity of cellulose-[DBNH][CO_2Et] solutions is more temperature sensitive and slightly more energy is needed to flow these solutions as compared to cellulose-[Emim][OAc].

Time-temperature superposition principle was applied to build master curves by shifting the experimental data of *G'*, *G"* and η^* by the corresponding a_T shift factor. The latter was calculated from the equation (3) with T_{ref} as the reference temperature, here 20 °C.

$$a_T = exp\left(\frac{E_a}{R}\left(\frac{1}{T} - \frac{1}{T_{ref}}\right)\right) \quad (3)$$

The examples of master plots for 8% and 5% cellulose-[DBNH][CO_2Et] solutions, all data reduced to the reference temperature of 20 °C, are shown in Figure 6. *G''* is higher than *G'* for both concentrations for five decades of frequency; these solutions behave as a classical unentangled polymer solution. For a monodispersed flexible polymer at low frequencies Maxwell model predicts power law exponents in $G' \sim \omega^x$ and $G'' \sim \omega^y$ as $x = 2$ and $y = 1$.For 8% solutions $x_{exp} = 1.85$ and $y_{exp} = 0.94$, and for 5% solutions $x_{exp} = 1.63$ and $y_{exp} = 0.99$. The values obtained show the applicability of Maxwell model in the terminal zone; a deviation for 5% solution may be due to the fact that terminal zone cannot be reached because of too low *G'* values.

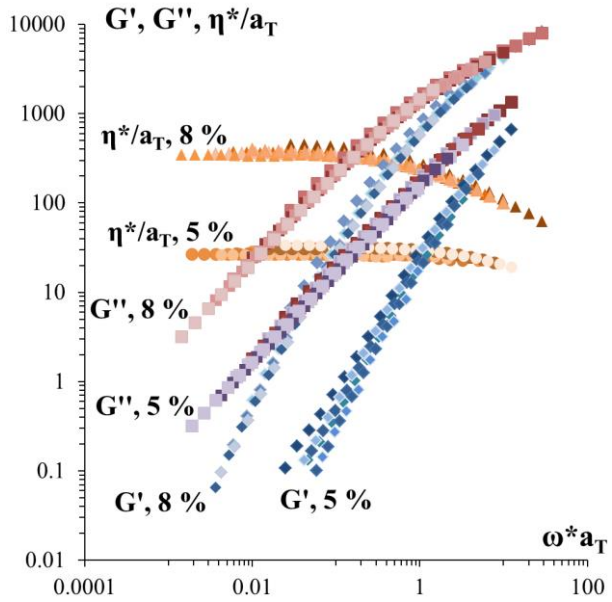

Figure 6.

Master curves for *G'*, *G''* and complex viscosity of 5% and 8% cellulose-[DBNH][CO_2Et] solutions at temperature ranging from 10 °C to 60 °C, with 20 °C as reference temperature.

3.1.4. Concentration dependences, intrinsic viscosity and overlap concentration

Figure 7 shows the influence of cellulose concentration on the Newtonian viscosity of solutions at different temperatures. Two different regions can be distinguished: the dilute region, with linear viscosity-concentration dependence, and the semi-dilute region that obeys the power law $\eta_N \sim C^n$. The power law coefficient *n* decreases with increasing temperature from 3.78 at 10 °C to 2.93 at 50 °C. Similar values and tendencies were already reported for cellulose in different ionic liquids and in other solvents.[45,49-51]

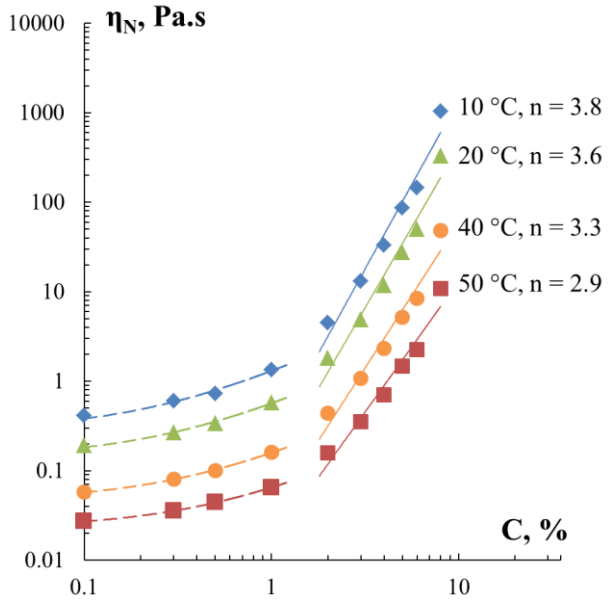

Figure 7.

Newtonian viscosity as a function of cellulose concentration at different temperatures. Dashed lines correspond to the linear dependence in dilute region and solids lines correspond to the power-law approximation above the overlap concentration, *n* is power law coefficient.

The intrinsic viscosity $[\eta]$ is an important parameter that describes the volume of macromolecule depending on temperature and thermodynamic quality of the solvent. Cellulose intrinsic viscosity in [DBNH][CO_2Et] was calculated using the Wolf approach.[52,53] This method was preferred over the classical Huggins approach for two main reasons: firstly, measurements in a capillary Ubbelohde viscometer were not possible because of the too high viscosity of our solutions and because of the solvent sensitivity to moisture and oxygen.

Secondly, when using the zero shear rate viscosity values calculated above, the Huggins plots where scattered and did not allow an adequate determination of the intrinsic viscosity. In Wolf approach,[52] according to phenomenological considerations, the calculation of the limiting slope of the logarithm of the relative viscosity (η_{rel}) versus concentration is identical to the intrinsic viscosity, where $\eta_{rel} = \eta_{sol}/\eta_{solv}$ with η_{sol} and η_{solv} being solution and solvent viscosities, respectively. This approach was developed for polyelectrolyte solutions but it was also successfully used for uncharged polymer solutions as shown by Eckelt et al. for cellulose dissolved in NMMO monohydrate.[53] This approach was also used to determine amylopectin intrinsic viscosity[54] and cellulose acetate intrinsic viscosity[55], both in [Emim][OAc]. Cellulose concentrations were recalculated in $mL.g^{-1}$, with mean value of [DBNH][CO_2Et] density taken for all solution concentrations as 1.1 $g.cm^{-3}$. It was shown that [DBNH][CO_2Et] density-temperature dependence is very weak[56] and may not be taken into account within experimental errors.

Figure 8 demonstrates the intrinsic viscosity of cellulose in [DBNH][CO_2Et] and in [Emim][OAc] as a function of temperature, the latter taken from Gericke et al. 2009.[45] Both intrinsic viscosities decrease with temperature increase. This shows that cellulose macromolecules are sensitive to temperature variations, and that thermodynamic quality of both solvents is decreasing with the increase of temperature. The intrinsic viscosity of cellulose in [DBNH][CO_2Et] is more than two times higher than that in [Emim][OAc], indicating that in this temperature range [DBNH][CO_2Et] is thermodynamically much better solvent of cellulose. For example, $[\eta]$ at 20 °C is 237 $mL.g^{-1}$ in [DBNH][CO_2Et] against 101 $mL.g^{-1}$ in [Emim][OAc].

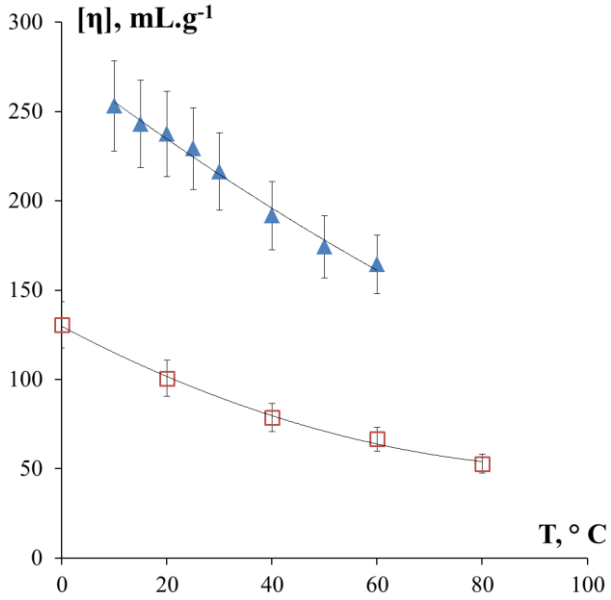

Figure 8.

Intrinsic viscosities of cellulose in [DBNH][CO_2Et] (filled points) and in [Emim][OAc] (openpoints, data taken from ref.45) as a function of temperature. Lines are given to guide the eye.

As mentioned above, cellulose overlap concentration is an important parameter which reflects the end of dilute regime; it can be roughly estimated as $C^* = 1/[\eta]$. According to results presented in Figure 8, cellulose overlap concentration in [DBNH][CO_2Et] is much lower than that in [Emim][OAc] in the temperature interval studied. For example, at 20 °C in [DBNH][CO_2Et] $C^* = 4.2.10^{-3}$ g.mL^{-1} (0.38%) and in [Emim][OAc] $C^* = 9.9.10^{-3}$ g.mL^{-1} (0.9%). This is an important result to take into account for processing because it means that cellulose network can be formed at lower cellulose concentrations when dissolved in [DBNH][CO_2Et]. It means that in order to make intact beads with JetCutter, cellulose concentration in [DBNH][CO_2Et] should be at least 1 wt%. The results on the beads obtained with JetCutting technology are presented in the next section.

3.2. Cellulose aerogel beads

3.2.1. Visual observations and size distribution

The images of cellulose aerogel beads made from 2 and 3% cellulose-[DBNH][CO_2Et] coagulated in water, ethanol and isopropanol are shown in Figure 9. Their size distribution together with mean arithmetic values of diameter ($\overline{D}$) and standard deviation (σ) are shown in Figure 10. Cellulose concentration plays the main role in the size and shape of the beads: mean diameter from 2% cellulose-[DBNH][CO_2Et] solution, whatever the coagulation bath, varies from 0.5 to 0.7 mm (Figure 10 a, b, c), and from 3% solution it is around 1.8 mm (Figure 10 d). The reason is that viscosity of 3% solution is more than two times higher than that of 2% solution at 20 °C: 1.8 Pa.s vs 4.9 Pa.s, respectively (Figure 7). These concentrations are in semi-dilute region with viscosity proportional to polymer concentration in power 3.6 at room temperature (Figure 7).

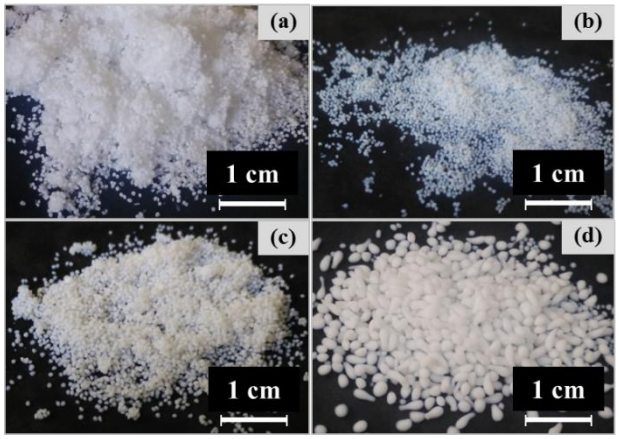

Figure 9.

Cellulose aerogel beads from 2% (a, b, c) and 3% (d) cellulose-[DBNH][CO_2Et] solutions coagulated in water (a), isopropanol (b) and ethanol (c, d).

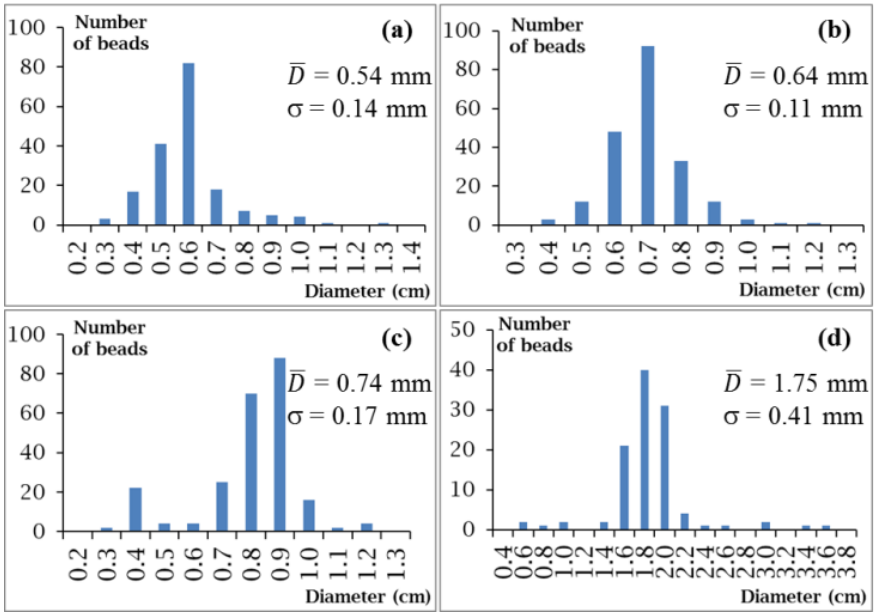

Figure 10.

Size distribution, mean diameter ($\overline{D}$) and standard deviation (σ) for aerogel beads as shown in Figure 9: cellulose aerogel beads from 2% (a, b, c) and 3% (d) cellulose-[DBNH][CO_2Et] solutions coagulated in water (a), isopropanol (b) and ethanol (c, d).

3.2.2. Bulk density, specific surface area and morphology

The main characteristics of aerogels such as bulk density, porosity, pore volume and specific surface area are shown in Table 1 for beads made from 2 and 3% cellulose-[DBNH][CO_2Et] solutions and coagulated in water, isopropanol and ethanol. Bulk densities are very low, 0.04 – 0.05 g.cm^{-3} for samples from 2% solutions, and 0.07 gcm^{-3} for samples from 3% solutions, but are still higher than what could be expected for the case of no volume change during all processing steps. The reason is shrinkage during solvent exchange which leads to non-solvent induced phase separation and also during drying (large difference between the solubility parameters of cellulose and CO_2). For the low cellulose concentrations used, shrinkage is around 60 – 70 vol% corresponding to previously reported results on

aerogel monoliths from cellulose-[Emim][OAc] solutions.[7] It seems that the type of coagulation bath does not influence much the density within the interval of conditions studied.

Table 1. Bulk density, porosity, specific surface area and specific pore volume of cellulose aerogel beads made from 2 and 3% solutions and coagulated in water, isopropanol and ethanol

Cellulose concentration, %	Coagulation bath	Bulk density, $g.cm^{-3}$	Porosity, %	Specific surface area, $m^2.g^{-1}$	Specific pore volume, $cm^3.g^{-1}$
2	water	0.04	97.3	238	24.3
2	isopropanol	0.04	97.3	302	24.3
2	ethanol	0.05	96.7	295	19.3
3	ethanol	0.07	95.3	257	13.6

Porosity was calculated using the values of bulk density, ρ_{bulk}, and cellulose skeletal density, which is the same as for neat cellulose, ρ_{sk} = 1.5 $g.cm^{-3}$.[30,57]

$$Porosity, \% = 1 - \frac{\rho_{bulk}}{\rho_{sk}} \times 100\% \quad (4)$$

As expected from low values of bulk density, porosity is very high, from 95 to 97% (Table 1). Specific surface area, S_{BET}, is within 240 – 300 $m^2.g^{-1}$ for all aerogel beads, which reflects certain mesoporosity. Overall, density and specific surface area of cellulose aerogel beads are very similar to those obtained for aerogel monoliths from ionic liquids, NMMO monohydrate and NaOH-water based solvents.[1,3,5,6,8,9] JetCutting technology preserves the main characteristics of cellulose aerogels.

The experimental results presented in Table 1 allowed a rough estimation of the theoretical specific pore volume V_{pores}:

$$V_{pores} = \frac{1}{\rho_{bulk}} - \frac{1}{\rho_{sk}} \quad (5)$$

The results are shown in Table 1. Pore volume is high and comparable with that of other bio-aerogels.[14] It should be noted that pore volume and pore size distribution of bio-aerogels with "mixed" meso- and macro-porosity cannot be measured with nitrogen adsorption and BJH approach: the experimental data take into account only 10-20% of the real volume. This was demonstrated for several bio-aerogels.[14, 57-59] Mercury porosimetry also does not allow measuring pore size distribution as far as sample are compressed and mercury does not penetrate the pores; the result recorded is thus an artefact.[13, 57]

The internal morphology of aerogel beads is presented in Figure 11. All samples are with small and large macropores and some mesoporosity as reflected by specific surface area.

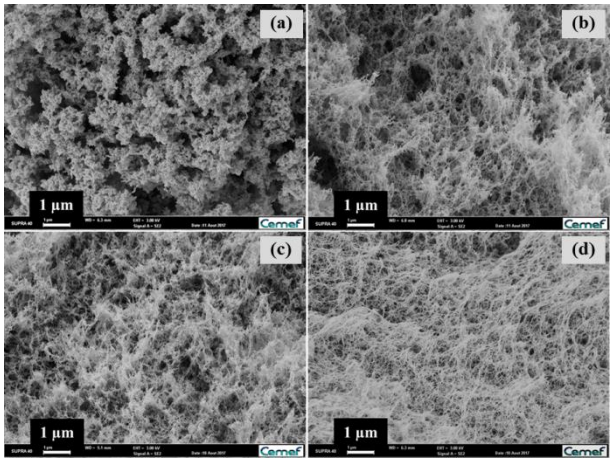

Figure 11. Morphology of aerogel beads from cellulose-[DBNH][CO_2Et] solutions of 2% (a, b, c) and 3% (d) coagulated in water (a), isopropanol (b) and ethanol (c, d).

4. Conclusions

This work is an extended investigation of the rheological properties of cellulose-[DBNH][CO_2Et] solutions in the view of using these results for making cellulose aerogel

beads with JetCutting technology and drying with supercritical CO_2. The flow and viscoelastic properties of cellulose-[DBNH][CO_2Et] solutions were studied as a function of polymer concentration and solution temperature. In the range of conditions used all solutions show Newtonian plateau with a beginning of shear thinning regime for higher cellulose concentrations and lower temperatures. Viscoelastic properties of cellulose-[DBNH][CO_2Et] solutions can be described by classical approaches used in polymer physics. Cellulose intrinsic viscosity in [DBNH][CO_2Et] turned out to be more than two times higher than that in previously studied [Emim][OAc] solutions for the same cellulose, and also decreases with temperature increase. Thermodynamic quality of [DBNH][CO_2Et] is thus higher at the same temperature leading to more swollen polymer coils and lower overlap concentration. The latter allowed fitting into the processing window of JetCutter in terms of not too high viscosity but high enough cellulose concentration to make intact beads.

Aerogel beads were prepared from 2 and 3% of cellulose-[DBNH][CO_2Et] solutions by replacing ionic liquid by water, ethanol or isopropanol followed by drying with supercritical CO_2. Cellulose concentration was the major factor controlling beads' size which varied from 0.5 – 0.7 mm when made from 2% solutions to 1.7 mm from 3% solution. The density of beads was 0.04 – 0.07 $g.cm^{-3}$ and specific surface area 240 – 340 $m^2.g^{-1}$. We demonstrated that by a careful selection of solution properties it is possible to obtain with JetCutting technology intact cellulose aerogel beads with properties similar to those known for monolithic cellulose aerogels made using other solvents. The results can be extended for making other bio-aerogels in the form of beads. This opens numerous opportunities for using bio-aerogels, and in particular cellulose aerogel beads, as carriers for controlled release applications in cosmetics, food and pharma.

Acknowledgments

Authors express their great thanks to Dr. Alistair King, university of Helsinki, Finland, for the guidance in the synthesis of [DBNH][CO_2Et] and for performing high-resolution NMR spectra. This project has received funding from the European Union´s Horizon 2020 research and innovation program under grant agreement No 685648.

References

1 R. Gavillon and T. Budtova, *Biomacromolecules*, 2008, **9**, 269–277.

2 R. Sescousse, R. Gavillon and T. Budtova, *J. Mater. Sci.*, 2010, **46**, 759–765.

3 C. Tsioptsias, A. Stefopoulos, I. Kokkinomalis, L. Papadopoulou and C. Panayiotou, *Green Chem.*, 2008, **10**, 965.

4 M. Deng, Q. Zhou, A. Du, J. van Kasteren and Y. Wang, *Mater. Lett.*, 2009, **63**, 1851–1854.

5 O. Aaltonen and O. Jauhiainen, *Carbohydr. Polym.*, 2009, **75**, 125–129.

6 R. Sescousse, R. Gavillon and T. Budtova, *Carbohydr. Polym.*, 2011, **83**, 1766–1774.

7 N. Buchtova and T. Budtova, *Cellulose*, 2016, **23**, 2585–2595.

8 J. Innerlohinger, H. K. Weber and G. Kraft, *Macromol. Symp.*, 2006, **244**, 126–135.

9 F. Liebner, A. Potthast, T. Rosenau, E. Haimer and M. Wendland, *Holzforschung*, 2008, **62**, 129-135.

10 B. J. C. Duchemin, M. P. Staiger, N. Tucker and R. H. Newman, *J. Appl. Polym. Sci.*, 2010, **115**, 216–221.

11 H. Jin, Y. Nishiyama, M. Wada and S. Kuga, *Colloids Surf. Physicochem. Eng. Asp.*, 2004, **240**, 63–67.

12 M. Schestakow, I. Karadagli and L. Ratke, *Carbohydr. Polym.*, 2016, **137**, 642–649.

13 C. A. García-González, J. J. Uy, M. Alnaief and I. Smirnova, *Carbohydr. Polym.*, 2012, **88**, 1378–1386.

14 C. Rudaz, R. Courson, L. Bonnet, S. Calas-Etienne, H. Sallée and T. Budtova, *Biomacromolecules*, 2014, **15**, 2188–2195.

15 A. Veronovski, G. Tkalec, Ž. Knez and Z. Novak, *Carbohydr. Polym.*, 2014, **113**, 272–278.

16 F. Quignard, R. Valentin and F. D. Renzo, *New J. Chem.*, 2008, **32**, 1300–1310.

17 P. Gurikov, S. P. Raman, D. Weinrich, M. Fricke and I. Smirnova, *RSC Adv*, 2015, **5**, 7812–7818.

18 F. Liebner, E. Haimer, M. Wendland, M.-A. Neouze, K. Schlufter, P. Miethe, T. Heinze, A. Potthast and T. Rosenau, *Macromol. Biosci.*, 2010, **10**, 349–352.

19 M. Pääkkö, J. Vapaavuori, R. Silvennoinen, H. Kosonen, M. Ankerfors, T. Lindström, L. A. Berglund and O. Ikkala, *Soft Matter*, 2008, **4**, 2492.

20 Y. Kobayashi, T. Saito and A. Isogai, *Angew. Chem. Int. Ed.*, 2014, **53**, 10394–10397.

21 J. Lee and Y. Deng, *Soft Matter*, 2011, **7**, 6034-6040.

22 D.-Y. Zhang, N. Zhang, P. Song, J.-Y. Hao, Y. Wan, X.-H. Yao, T. Chen and L. Li, *Carbohydr. Polym.*, 2018, **181**, 560–569.

23 Y.-X. Bai and Y.-F. Li, *Carbohydr. Polym.*, 2006, **64**, 402–407.

24 P. Rosenberg, I. Suominen, M. Rom, J. Janicki and P. Fardim, *Cellul. Chem. Technol.*, 2007, **41**, 243–254.

25 W. De Oliveira and W. G. Glasser, *J. Appl. Polym. Sci.*, 1996, **60**, 63–73.

26 J. Trygg, E. Yildir, R. Kolakovic, N. Sandler and P. Fardim, *Cellulose*, 2014, **21**, 1945–1955.

27 J. Trygg, P. Fardim, M. Gericke, E. Mäkilä and J. Salonen, *Carbohydr. Polym.*, 2013, **93**, 291–299.

28 X. Luo and L. Zhang, *J. Chromatogr. A*, 2010, **1217**, 5922–5929.

29 C. Lin, H. Zhan, M. Liu, S. Fu and L. A. Lucia, *Langmuir*, 2009, **25**, 10116–10120.

30 S. M. Kamal Mohamed, K. Ganesan, B. Milow and L. Ratke, *RSC Adv*, 2015, **5**, 90193–90201.

31 M. Braun, N. Guentherberg, M. Lutz, A. Magin, M. Siemer, V. N. Swaminathan, B. Linner, F. Ruslim and R. G. Fernandez US Pat., 2010331222 (A1), 2010.

32 L. K. Voon, S. C. Pang and S. F. Chin, *Materials Letters*, 2016, **164**, 264–266.

33 M. Gericke, J. Trygg and P. Fardim, *Chem. Rev.*, 2013, **113**, 4812–4836.

34 O. A. El Seoud, A. Koschella, L. C. Fidale, S. Dorn and T. Heinze, *Biomacromolecules*, 2007, **8**, 2629–2647.

35 Y. Ma, S. Asaadi, L. S. Johansson, P. Ahvenainen, M. Reza, M. Alekhina, L. Rautkari, A. Michud, L. Hauru, M. Hummel and H. Sixta, *ChemSusChem*, 2015, **8**, 4030–4039.

36 T. Budtova, P. Navard, *Cellulose*, 2016, 23, 5–55.

37 T. C. R. Brennan, S. Datta, H. W. Blanch, B. A. Simmons and B. M. Holmes, *BioEnergy Research*, 2010, **3**, 123–133.

38 K. E. Gutowski, G. A. Broker, H. D. Willauer, J. G. Huddleston, R. P. Swatloski, J. D. Holbrey and R. D. Rogers, *J. Am. Chem. Soc., 2003*, **125**, 6632–6633.

39 K. Shill, S. Padmanabhan, Q. Xin, J. M. Prausnitz, D. S. Clark and H. W. Blanch, *Biotechnol. Bioeng.*, 2011, **108**, 511–520.

40 A. W. T. King, A. Parviainen, P. Karhunen, J. Matikainen, L. K. J. Hauru, H. Sixta and I. Kilpeläinen, *RSC Adv.*, 2012, **2**, 8020–8026.

41 A. W. T. King, J. Asikkala, I. Mutikainen, P. Järvi and I. Kilpeläinen, *Angew. Chem. Int. Ed.*, **2011**, 50, 6301–6305.

42 A. Parviainen, A. W. T. King, I. Mutikainen, M. Hummel, C. Selg, L. K. J. Hauru, H. Sixta and I. Kilpeläinen, *ChemSusChem*, 2013, 6, 2161–2169.

43 A. Parviainen, R. Wahlstrom, U. Liimatainen, T. Liitia, S. Rovio, J. K. J. Helminen, U. Hyvakko, A. W. T. King, A. Suurnakki and I. Kilpelainen, *RSC Adv.*, 2015, **5**, 69728–69737.

44 R. Gavillon, PhD thesis, École Nationale Supérieure des Mines de Paris, 2007.

45 M. Gericke, K. Schlufter, T. Liebert, T. Heinze and T. Budtova, *Biomacromolecules*, 2009, **10**, 1188–1194.

46 M. Gericke, T. Liebert, O. A. El Seoud and T. Heinze, *Macromol. Mater. Eng.*, 2011, **296**, 483–493.

47 K. A. Le, C. Rudaz and T. Budtova, *Carbohydr. Polym.*, 2014, **105**, 237–243.

48 W. P. Cox and E. H. Merz, *J. Polym. Sci.*, 1958, **28**, 619–622.

49 R. Sescousse, K. A. Le, M. E. Ries and T. Budtova, *J. Phys. Chem. B*, 2010, **114**, 7222–7228.

50 J.-F. Blachot, N. Brunet, P. Navard and J.-Y. Cavailles, *Rheol. Acta*, 1998, **37**, 107–114.

51 T. Matsumoto, D. Tatsumi, N. Tamai and T. Takaki, *Cellulose*, 2001, **8**, 275–282.

52 B. A. Wolf, *Macromol. Rapid Commun.*, 2007, **28**, 164–170.

53 J. Eckelt, A. Knopf, T. Röder, H. K. Weber, H. Sixta and B. A. Wolf, *J. Appl. Polym. Sci.*, 2011, **119**, 670–676.

54 W. Liu and T. Budtova, *Carbohydr. Polym.*, 2013, **93**, 199–206.

55 C. Rudaz and T. Budtova, *Carbohydr. Polym.*, 2013, **92**, 1966–1971.

56 S. M. Green, PhD thesis, University of Leeds, 2017.

57 C. Rudaz, PhD thesis, Mines ParisTech, 2013.

58 C. Jiménez-Saelices, B. Seantier, B. Cathala and Y. Grohens, *Carbohydr. Polym.*, 2017, **157**, 105–113.

59. M. Robitzer, F. Di Renzo and F. Quignard, *Microporous and Mesoporous Materials*, 2011, **140**, 9–16.

Supporting Information

Rheology of cellulose-[DBNH][CO_2Et] solutions and shaping into aerogel beads

Lucile Druel[1], Philipp Niemeyer[2], Barbara Milow[2], Tatiana Budtova[1]*

[1] *MINES ParisTech, PSL Research University, Centre for Material Forming (CEMEF), UMR CNRS 7635, CS 10207, 06904 Sophia Antipolis, France*

[2] *Deutsches Zentrum für Luft- und Raumfahrt Institut für Werkstoff-Forschung, Abteilung Aerogele, Linder Höhe, 51147 Köln, Germany*

Figure S1.

^{1}H NMR in DMSO-d_6 full (a) and expanded (b) spectra of [DBNH][CO_2Et] with main peak assignments in ppm (a) and with all peak assignments (b)

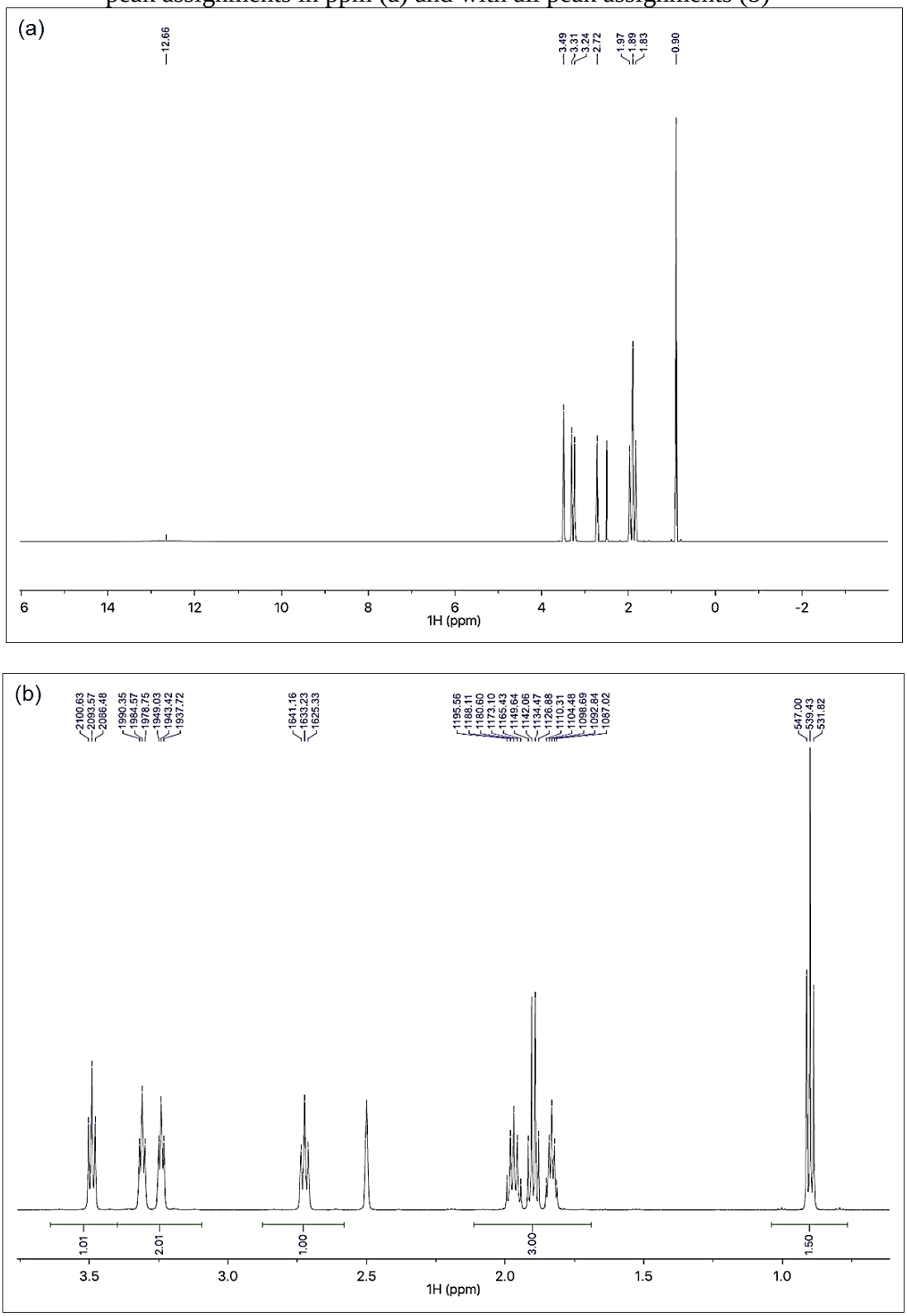

^{1}H NMR (600 MHz, DMSO-d_6, 27 °C): δ 0.90 (t, *J* = 7.6 Hz, 3H), 1.83 (m, 2H), 1.89 (q, *J* = 7.6 Hz, 2H), 1.97 (m, 2H), 2.72 (t, *J* = 7.9 Hz, 2H), 3.24 (t, *J* = 5.7 Hz, 2H), 3.31 (t, *J* = 5.8 Hz,2H), 3.49 (t, *J* = 7.1 Hz, 2H), 12.66 (br s, 1H).

Figure S2.

Pictures of the JetCutter (right) and one of the cutting tool used (bottom left)